Siberian Branch of Russian Academy of Science
BUDKER INSTITUTE OF NUCLEAR PHYSICS

D. Farina, I. Kotelnikov, R. Pozzoli

DYNAMICS OF FAST MAGNETOSONIC PERTURBATIONS CLOSE TO X–X SEPARATRIX

Budker INP 99-31

http://www.inp.nsk.su/publications

Novosibirsk
1999

Budker Institute of Nuclear Physics

D. Farina, I. Kotelnikov, R. Pozzoli

Dynamics of Fast Magnetosonic Perturbations Close to X–X Separatrix

BudkerINP 99–31

Novosibirsk
1999

DYNAMICS OF FAST MAGNETOSONIC PERTURBATIONS CLOSE TO X–X SEPARATRIX

D. Farina[1], *I. Kotelnikov, R. Pozzoli*[2]

Budker Institute of Nuclear Physics
630090, Novosibirsk, Russian Federation

Abstract

The structure of magnetosonic perturbations around a pair of X–lines of a toroidal magnetic configuration is analyzed in the framework of ideal MHD, by means of a WKB technique. The conditions for the wave trapping are investigated. It is shown that the wave equation for the displacement is separable in the vicinity of the X–lines. The relevant eigenvalues and the different types of ray trajectories are discussed.

[1]Istituto di Fisica del Plasma, Consiglio Nazionale delle Ricerche, EURATOM-ENEA-CNR Association, via Cozzi 53, 20125 Milano,Italy.

[2]Istituto Nazionale di Fisica della Materia, Dipartimento di Fisica, Università di Milano, via Celoria 16, 20133 Milano, Italy.

1. Introduction

When a magnetic configuration is modified by localized currents flowing into the plasma or in external coils, singular magnetic field lines may arise in the system, and affect the propagation of MHD waves. In particular, wave trapping inside the plasma can occur, giving rise to eigenmodes. We refer here to fast magnetoacoustic perturbations in the ideal MHD limit, in a uniform, currentless, zero β, unperturbed plasma.

We shall consider configurations with one cyclic coordinate (z), i.e., magnetic field of the form $\boldsymbol{B}(x,y) = B_z \boldsymbol{e}_z + \boldsymbol{B}_p(x,y)$, with constant B_z and $\boldsymbol{B}_p = \nabla\psi(x,y) \times \boldsymbol{e}_z$, with $\nabla^2\psi = 0$. An X–line is characterized by $\boldsymbol{B}_p = 0$. From $\nabla \times \boldsymbol{B}_p = 0$, it then follows that in its closest neighborhood the field lines are hyperbolic, when projected onto the x, y plane. Trapping of fast waves around an X–line has been considered in Ref. [1]. Here we extend the investigation to include the case of two close X–lines, which can be produced in various systems. This case is of relevance to the problem of magnetic reconnection (see e.g., the review in Ref. [2] and the recent investigation in Ref. [3]).

Different topologies of regular ray trajectories, and also stochastic trajectories are found. The analysis is made in the framework of the WKB method. The present model can be applied, e. g. to the case of divertor geometry. More generally, the present investigation is of interest for the problem of the hamiltonian motion of a single particle trapped in a 2D potential.

The paper is organized as follows. The WKB method of analysis is introduced in Sec.2. The case of a single X–line is presented in Sec. 3.1. The case of two close X–lines is analyzed in Sec. 3.2. Conclusions are given in Sec. 4.

2. Formulation of the problem

In the framework of ideal MHD the displacement vector $\boldsymbol{\xi}(x,y,z)$ for a stationary perturbation with frequency ω satisfies the wave equation

$$4\pi\rho\omega^2\boldsymbol{\xi} + \boldsymbol{B}\times\{\nabla\times[\nabla\times(\boldsymbol{B}\times\boldsymbol{\xi})]\} = 0\,, \qquad (1)$$

where ρ is the plasma density.

In the WKB approximation characterized by a formal smallness parameter ε, we look for asymptotic solutions in ε, superposition of functions of the form

$$\boldsymbol{\xi} = A(\boldsymbol{x})\exp(iS(\boldsymbol{x})/\varepsilon)\boldsymbol{\tau}\,, \qquad (2)$$

where S is the eikonal, A the amplitude, and the unit vector $\boldsymbol{\tau}(\boldsymbol{x})$ the polarization of the mode. The function S satisfies the Hamilton–Jacobi equation, which, introducing $\boldsymbol{k} = \nabla S$, can be written in the form

$$\lambda(\boldsymbol{x},\boldsymbol{k}) = 0\,, \qquad (3)$$

where λ plays the role of a ray Hamiltonian, and the ray trajectories are given by the Hamilton equations

$$\dot{\boldsymbol{x}} = \frac{\partial\lambda}{\partial\boldsymbol{k}}\,, \qquad \dot{\boldsymbol{k}} = -\frac{\partial\lambda}{\partial\boldsymbol{x}}\,.$$

For fast waves, we have [1,4]

$$\lambda = -4\pi\rho\omega^2 + k^2B^2\,, \qquad (4)$$

and the polarization $\boldsymbol{\tau}$ reads

$$\boldsymbol{\tau} = \frac{\boldsymbol{B}\times(\boldsymbol{B}\times\boldsymbol{k})}{|\boldsymbol{B}\times(\boldsymbol{B}\times\boldsymbol{k})|}\,. \qquad (5)$$

The amplitude A satisfies the transport equation

$$\frac{\partial}{\partial\boldsymbol{x}}\cdot\left(A^2\frac{\partial\lambda}{\partial\boldsymbol{k}}\right) = 0\,.$$

In the case of trapping, the eigenfrequencies are determined from the semiclassical quantization rule for the action

$$J_i = \frac{1}{2\pi}\oint_{C_i}\boldsymbol{k}\cdot d\boldsymbol{x} = n_i + \frac{1}{2}m_i\,, \qquad (6)$$

where C_i are independent circuits on the invariant torus, n_i the quantum numbers, and m_i the Maslov indexes.

In the configuration under consideration, λ does not depend on z, and k_z is a constant of motion. Since the system is periodic in z, $k_z = 2\pi n/L_z$, where n is integer, and L_z is the z–periodicity length.

To analyze the ray trajectories, it is convenient to use the following 2D Hamiltonian [4]

$$H(x,y,k_x,k_y) = \frac{1}{2}(k_x^2+k_y^2) + V(x,y) = 0 \qquad (7)$$

where $V(x,y) = [k_z^2 - 4\pi\rho\omega^2/B^2]/2$. At the surface $H=0$, it has the same trajectories as (4). This Hamiltonian corresponds to that of a 2D motion of a particle with kinetic energy $(k_x^2+k_y^2)/2$, and potential energy $V(x,y)$.

3. Magnetic field configuration and ray trajectories

3.1. Single X–line

Let us consider first the case of a single X–line. Referring to a divertor configuration, the magnetic field $\boldsymbol{B}_p$ around the separatrix can be described as that due to two equal currents flowing in two wires parallel to the z axis, located at $x = \pm L$ on the x axis. The corresponding flux function reads

$$\psi = \frac{B_{p0}L}{2}\ln\left[\frac{(x^2-y^2-L^2)^2+4x^2y^2}{L^4}\right], \qquad (8)$$

and the magnetic field amplitude $B = (B_z^2+B_p^2)^{1/2}$ where

$$B_p^2 = 4B_{p0}^2L^2\frac{x^2+y^2}{(x^2-y^2-L^2)^2+4x^2y^2}\,. \qquad (9)$$

In the following, dimensionless variables are used (without change of notation). In this section, length, magnetic field, and time are measured respectively in units of L, B_z, and $t_A = L/c_{A0}$, being $c_{A0} = B_z/\sqrt{4\pi\rho}$ the Alfvén speed in the field B_z. The field lines (contour plots of ψ), projected onto the x,y plane, and the contour plot of B^2 are shown in Figs. 1, 2. To analyze the ray trajectories, it is convenient to introduce elliptic coordinates μ, ν, so that

$$x = \cosh\mu\sin\nu\,, \qquad y = \sinh\mu\cos\nu\,, \qquad (10)$$

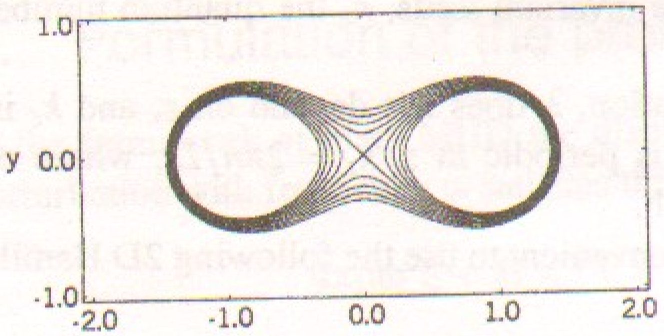

Figure 1. Contours of the flux function ψ, defined by Eq. (8) with $L = 1$, in the x, y plane. The X–point is located at $x = 0$, $y = 0$.

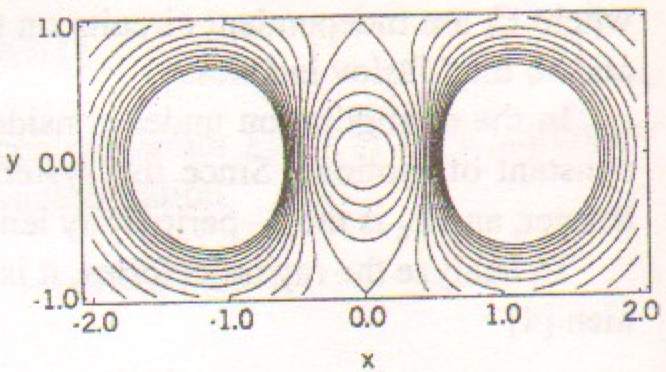

Figure 2. Contours of constant magnetic amplitude B^2, defined by Eq. (9) with $L = 1$, in the x, y plane. Note that $B_p^2 = 0$ at the point $x = 0$, $y = 0$.

and

$$B_p^2 = \alpha^2 \frac{S^2+s^2}{(C^2-s^2)^2}\,, \tag{11}$$

where $\alpha^2 = 4B_{p0}^2/B_z^2$, $S = \sinh\mu$, $C = \cosh\mu$, $s = \sin\nu$, and $c = \cos\nu$.

Separability of the Hamiltonian can be easily obtained in the limit $B_p^2 \ll B_z^2$ in the neighborhood of the X–line, $\sinh^2\mu \ll 1$, and $\sin^2\nu \ll 1$. The potential V then reads

$$V(\mu,\nu) = \frac{-(\omega^2-k_z^2)(C^2-s^2)+\alpha^2\omega^2(S^2+s^2-S^4+s^4)}{2(C^2-s^2)}$$

By means of a canonical transformation with generatrix function $F(k_x,k_y;\mu,\nu) = -k_x x(\mu,\nu) - k_y y(\mu,\nu)$, the Hamiltonian takes the form

$$H(\mu,\nu,k_\mu,k_\nu) = \frac{k_\mu^2+k_\nu^2-(\omega^2-k_z^2)(C^2-s^2)+\alpha^2\omega^2(S^2+s^2-S^4+s^4)}{2(C^2-s^2)}\,. \tag{12}$$

Separability gives the following conditions

$$k_\nu^2 + (\omega^2-k_z^2)s^2 + \alpha^2\omega^2(s^2+s^4) = \beta\,. \tag{13a}$$

$$k_\mu^2 - (\omega^2-k_z^2)C^2 + \alpha^2\omega^2(S^2-S^4) = -\beta\,, \tag{13b}$$

where β is a constant.

Trapped trajectories exist provided that $\beta > 0$ and $k_z^2 < \omega^2 < k_z^2/(1-\alpha^2)$, cf. Ref. [1]. The caustics which bound the trajectories are determined by the conditions $k_\nu = 0$, $k_\mu = 0$, and coincide with the coordinate lines $\nu = const$, $\mu = const$. An example of ray trajectory is shown in Fig. 3. From Eqs. (13a, 13b) and the quantization rule (6) the eigenfrequencies are easily determined.

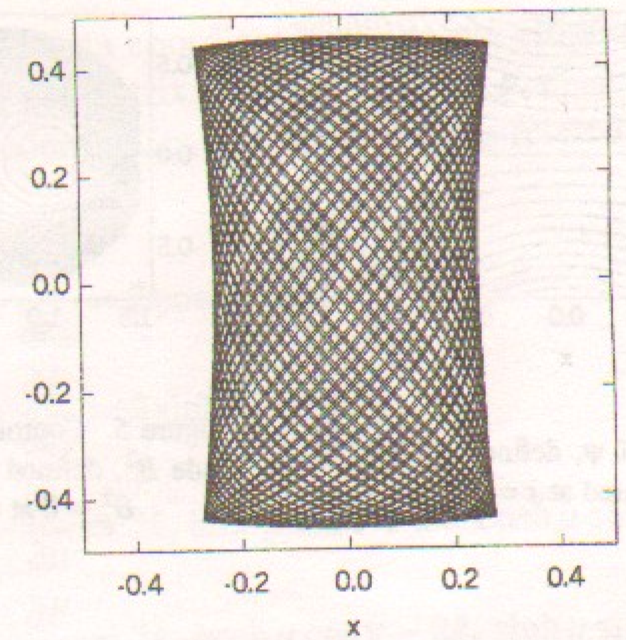

Figure 3. Example of a ray trajectory, projected in the (x,y) plane, trapped near the single X–point, for $\alpha^2 = 0.05$, $\beta/k_z^2 = 0.01$, and $\omega^2/k_z^2 = 1.01$. The trapping region is almost rectangular in the elliptic coordinates defined by Eq. (10).

3.2. Two close X–lines

We consider now a configuration characterized by two close X–lines. It can be realized in a divertor geometry by means of two external toroidal coils. In our model, we refer to a poloidal field $\mathbf{B}_p$ made by the superposition of a uniform field $-B_{0x}\mathbf{e}_x$, simulating the contribution of the plasma core in the divertor region, and a field $\mathbf{B}_1$, similar to that of previous section, produced by two equal currents, flowing in two parallel coils, along z, located at $x = \pm L$, $y = 0$. At the midplane $x = 0$, $\mathbf{B}_1$ has only the x component which is equal to $B_{1x}(0,y) = 2B_{p0}Ly/(L^2+y^2)$. The function $B_{1x}(0,y)$ has two extrema $\pm B_{p0}$ at $y = \pm L$. We are interested in the conditions, where B_{p0} is such that B_{0x} almost balances the field B_{1x} at the extremum $y = L$ ($B_{0x} \approx B_{p0}$), so that $\mathbf{B}_p$ in a small vicinity of this point is small, $|B_{0x} - B_{p0}| \ll B_{p0}$. In this region, instead of exact formulae for the magnetic field, we can use its expansion into the Taylor series. Then the flux function ψ reads

$$\psi = (B_{p0} - B_{0x})y + (B_{p0}/6L^2)(3x^2y - y^3) \tag{14}$$

where the coordinate y is now and henceforth counted from the former point $y = L$. Neglected terms here are provided that $x^2+y^2 \ll L^2$. In what follows we shall use $\bar{B} = |B_{p0} - B_{0x}|$ as the unit of measure of the magnetic field and $l = \sqrt{2|B_{0x}/B_{p0} - 1|}$ as the unit length, and assume $l \ll L$. The unit time is l/c_{A0}. In dimensionless units,

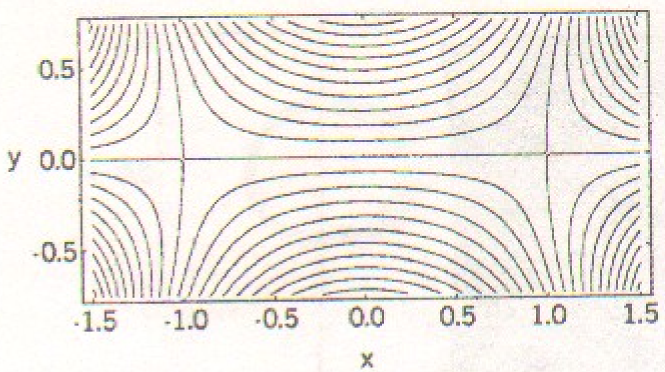

Figure 4. Contours of ψ, defined by Eq. (15), X–points are located at $x=\pm 1$, $y=0$.

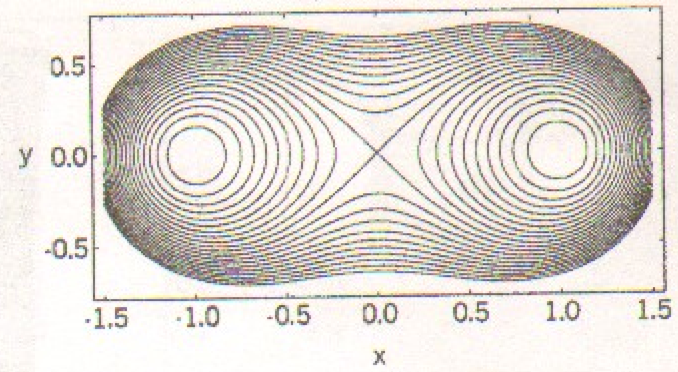

Figure 5. Contours of constant magnetic amplitude B^2, defined by Eq. (17), in the x, y plane. $B_p^2 = 0$ at the points $x=\pm 1$, $y=0$.

Eq. (14) reads

$$\psi = \pm y + \frac{1}{3}(3x^2 y - y^3)\,, \qquad (15)$$

where the plus and minus signs stand for the cases where $B_{p0} > B_{0x}$, and $B_{p0} < B_{0x}$, respectively.

The poloidal magnetic field derived from the flux function (15) has the following components:

$$B_x = \pm 1 + x^2 - y^2\,, \qquad B_y = -2xy\,. \qquad (16)$$

This configuration has two magnetic field nulls in $x=0$, $y=\pm 1$ (in the case of the upper sign), and in $x=\pm 1$, $y=0$ (in the the case of the lower sign) The poloidal magnetic field amplitude B_p^2 is given by

$$B_p^2 = \pm 2(x^2-y^2) + (x^2+y^2)^2 + 1\,. \qquad (17)$$

The corresponding field lines (contour plots of ψ), projected onto the x,y plane, and the contour plot of B_p^2 are shown in Figs. 4, 5 for the case with minus sign in Eqs. (15) and (17). It is easy to see that the map of the configuration with the plus sign can be produced from that with the minus sign simply rotating the system of coordinates by a right angle. Therefore, below we concentrate on one configuration only, and choose the minus signs in Eqs. (15) and (17). All the obtained results can be translated to the other configuration with minor, and obvious changes.

The relevant potential energy, for $B_p^2 \ll B_z^2$, then reads

$$V(x,y) \approx \frac{1}{2}\left[-(\omega^2 - k_z^2) + \alpha^2\omega^2[1 - 2(x^2-y^2) + (x^2+y^2)^2]\right]\,,$$

where now $\alpha \equiv \bar{B}/B_z \ll 1$.

Let's transform the Cartesian coordinates x, y to the elliptical coordinates μ, ν by means of the following generatrix function $F(k_x,k_y;\mu,\nu) = -2k_x\cosh\mu\sin\nu - 2k_y\sinh\mu\cos\nu$. The new coordinates and momenta are related to the old ones by means of

$$\begin{aligned} x &= -\frac{\partial F}{\partial k_x} = 2\cosh\mu\sin\nu\,, \\ y &= -\frac{\partial F}{\partial k_y} = 2\sinh\mu\cos\nu\,, \\ k_\mu &= -\frac{\partial F}{\partial \mu} = 2k_x\sinh\mu\sin\nu + 2k_y\cosh\mu\cos\nu\,, \\ k_\nu &= -\frac{\partial F}{\partial \nu} = 2k_x\cosh\mu\cos\nu - 2k_y\sinh\mu\sin\nu\,. \end{aligned}$$

The coordinate μ takes values from 0 to ∞, and ν varies from 0 to 2π. The new Hamiltonian reads

$$H(\mu,\nu,k_\mu,k_\nu) = \frac{k_\mu^2 + k_\nu^2 + U(\eta) - U(\xi)}{8(\xi^2-\eta^2)}\,, \qquad (18)$$

where $\xi = \cosh\mu$ $(\xi \geq 1)$, $\eta = \sin\nu$ $(-1 \leq \eta \leq 1)$, $U(q) = 4q^2[\omega^2 - k_z^2 - \alpha^2\omega^2(4q^2-3)^2]$. The separability condition now reads

$$k_\nu^2 + 4\eta^2[\omega^2 - k_z^2 - \alpha^2\omega^2(4\eta^2-3)^2] = \beta\,, \qquad (19a)$$

$$k_\mu^2 - 4\xi^2[\omega^2 - k_z^2 - \alpha^2\omega^2(4\xi^2-3)^2] = -\beta\,. \qquad (19b)$$

As already noted, the boundary of a trapping region consists of pieces of coordinate lines $\mu=$ const, and $\nu=$ const, since the ray motion is separable in the elliptic coordinates. Hence, at any point at the boundary one of the conditions

$$k_\nu(\eta,\omega,\beta) = 0\,, \qquad (20a)$$

$$k_\mu(\xi,\omega,\beta) = 0 \qquad (20b)$$

must be met. These equations are cubic in ξ^2 and η^2, so that boundary values of ξ and η can be expressed as functions of β. It is easier, however, to express the boundary value $\bar{\eta}$ of η through the boundary value $\bar{\xi}$ of ξ. Indeed, since Eq. (20a) actually coincides with Eq. (20b), we know that one of its three roots (with respect

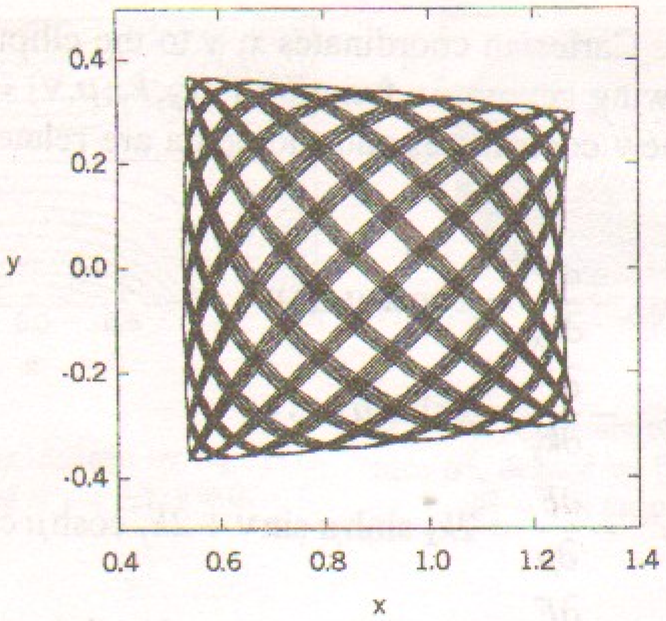

Figure 6. Example of a ray trajectory, projected in the (x,y) plane, for the case $0 < \Omega < 1/8$. The trajectories are trapped near the X–points in one or another half-planes. The particular trajectory shown here is obtained for the parameters $\alpha^2 = 0.05$, $\beta = -1$, $\Omega = 0.1$. The trapping region is rectangular in the elliptic coordinates defined by Eqs. (3.2).

to η^2) is equal to $\bar{\xi}^2$. This allows us to reduce Eq. (20a) to a second order algebraic equation in η^2:

$$2(\eta^4 + \eta^2\bar{\xi}^2 + \bar{\xi}^4) - 3(\eta^2 + \bar{\xi}^2) + (9/8 - \Omega) = 0\,, \qquad (21)$$

where $\Omega = [\omega^2 - k_z^2]/8\alpha^2\omega^2$, while $\bar{\xi}^2$ can take values larger than 1. The roots of Eq. (21)

$$\eta^2 = \frac{1}{4}(3 - 2\bar{\xi}^2) \pm \frac{1}{2}\sqrt{2\Omega - 3\bar{\xi}^2(\bar{\xi}^2 - 1)}\,, \qquad (22)$$

are real provided that $\Omega \geq 0$. This shows that magnetosonic waves can be trapped when $\omega^2 > k_z^2$.

As far as $\Omega < \frac{1}{8}$, the trajectories are trapped either in one or in the other half-plane (both roots are less than 1 but larger then 0). The case $0 < \Omega < \frac{1}{8}$ is shown in Fig. 6. If $\frac{1}{8} \leq \Omega \leq \frac{9}{8}$ two kinds of trajectories can exist. The ξ boundary may vary from $\bar{\xi}^2 = 1$ to $\bar{\xi}^2 = \frac{1}{2} + \sqrt{\frac{1}{4} + \frac{2}{3}\Omega}$. If $1 \leq \bar{\xi}^2 \leq \frac{3}{4} + \sqrt{\frac{1}{2}\Omega}$ trajectories reside in both halves of the x, y plane. If $\frac{3}{4} + \sqrt{\frac{1}{2}\Omega} < \bar{\xi}^2 \leq \frac{1}{2} + \sqrt{\frac{1}{4} + \frac{2}{3}\Omega}$ the trajectories are still trapped in one on the halves. The case $\frac{1}{8} \leq \Omega \leq \frac{9}{8}$ is shown in Fig. 7.

If $\Omega > \frac{9}{8}$, also two kinds of trajectories exist. The ξ boundary varies from $\bar{\xi}^2 = 1$ to $\bar{\xi}^2 = \frac{3}{4} + \sqrt{\frac{1}{2}\Omega}$. When $\frac{1}{4} + \sqrt{\frac{1}{2}\Omega} < \bar{\xi}^2 < \frac{3}{4} + \sqrt{\frac{1}{2}\Omega}$, trapped trajectories reside in

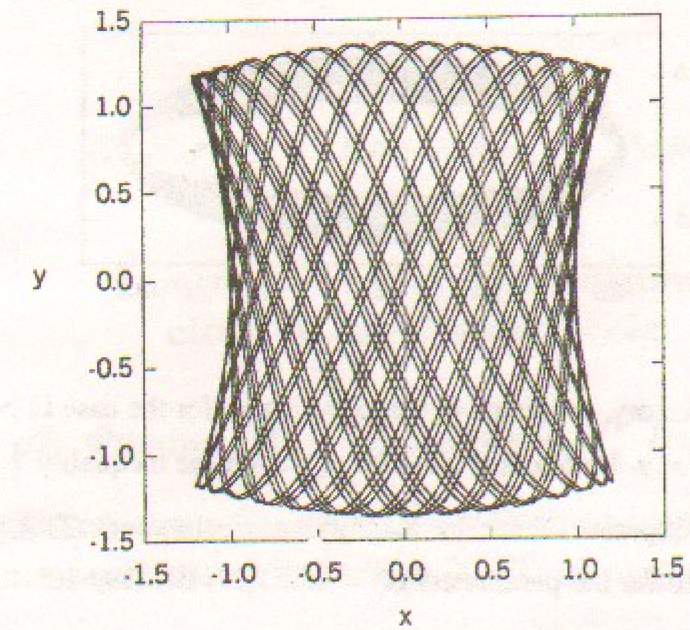

Figure 7. Example of a ray trajectory, projected in the (x,y) plane, for the case $1/8 < \Omega < 9/8$. The trajectories reside in both halves of x, y plane provided that the outer boundary $\bar{\xi}$ match the inequality $1 \leq \bar{\xi}^2 \leq \frac{3}{4} + \sqrt{\frac{1}{2}\Omega}$, otherwise they are trapped around one of the X–points $x = \pm 1$, $y = 0$. The particular trajectory shown here is obtained for the parameters $\alpha^2 = 0.05$, $\beta = 5$, $\Omega = 1.1$.

both halves of the x-y plane (larger of two roots of Eq. (22) is smaller than 1 while the smaller one is negative). When $\frac{1}{2} + \frac{1}{4}\sqrt{1 + \frac{8}{3}\Omega} < \bar{\xi}^2 < \frac{1}{4} + \sqrt{\frac{1}{2}\Omega}$ the larger of two roots (22) becomes greater than 1 so that the motion is unbounded in ν. This root gives another (inner) boundary in ξ^2 (which is in the range $1 < \bar{\xi}^2 < \frac{1}{2} + \frac{1}{4}\sqrt{1 + \frac{8}{3}\Omega}$) so that trapped trajectories are separated from the minima of magnetic field thus representing a sort of rotating trajectories. The latter case is shown in Fig. 8.

A similar classification of trajectories, referring to star orbits in galaxies, can be found, e.g., in Ref. [5].

4. Conclusions

We have investigated the trapping of fast magneto-acoustic perturbations in a magnetic configuration with z–periodicity, and exhibiting two close X lines. This type of configuration occurs in laboratory and astrophysical plasmas, and is of particular interest for the problem of magnetic reconnection.

We have shown the existence of well defined eigenmode system in the vicinity of the X–lines and have computed the eigenfrequencies in the WKB limit. We have identified different type of regular ray trajectories, and classified them according to the values of the parameter Ω and the linear dimension of the caustic $\bar{\xi}$. Stochastic

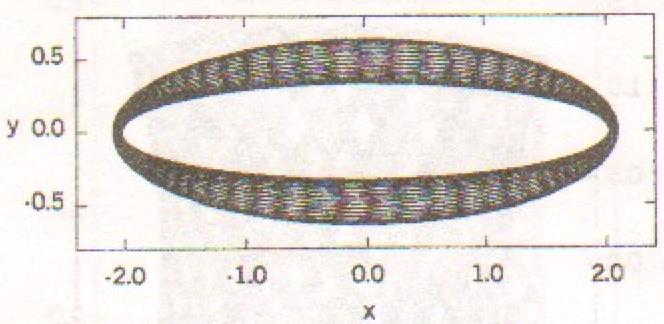

Figure 8. Example of a ray trajectory, projected in the (x, y) plane, for the case $\Omega > 9/8$. The trajectories always reside in both halves of x, y. If the outer boundary $\bar{\xi}$ match the inequality $\frac{1}{2}+\frac{1}{4}\sqrt{1+\frac{8}{3}\Omega} < \bar{\xi}^2 < \frac{1}{4}+\sqrt{\frac{1}{2}\Omega}$, the trajectories are separated from the X–points $x = \pm 1$, $y = 0$. This particular trajectory is obtained for the parameters $\alpha^2 = 0.05$, $\beta = 64$, $\Omega = 1.5$.

trajectories have also been found, and will be discussed in a future paper.

References

[1] D. Farina, A. Nassigh, R. Pozzoli, Physica Scripta, **T63**, 203 (1996); D. Farina, R. Pozzoli, Phys. Rev. E, **55**, 5909 (1997).

[2] D. Biskamp, *Nonlinear Magnetohydrodynamics*, Cambridge University Press, 1993.

[3] S.D. Bulanov, V.V. Pichushkin, K. Schindler, Plasma Phys. Reports, **22**, 887 (1996).

[4] S. Weinberg, Phys. Rev., **126**, 1899 (1962).

[5] Tim de Zeeuw, Mon. Not. Roy. Astron. Soc., **216**, 273 (1985).

D. Farina, I. Kotelnikov, R. Pozzoli

Dynamics of fast magnetosonic perturbations close to X–X separatrix

Д. Фарина, И. Котельников, Р. Поццали

Динамика быстрых магнито-звуковых возмущений вблизи X–X сепаратрисы

Budker INP 99-31

Ответственный за выпуск А.М. Кудрявцев
Работа поступила 18.03. 1999 г.

Сдано в набор 19.03.1999 г.
Подписано в печать 19.03.1999 г.
Формат бумаги 60×90 1/16 Объем 0.9 печ.л., 0.8 уч.-изд.л.
Тираж 120 экз. Бесплатно. Заказ N° 31

Обработано на IBM PC и отпечатано на
ротапринте ИЯФ им. Г.И. Будкера СО РАН
Новосибирск, 630090, пр. академика Лаврентьева, 11.